

- 14, 388 (1969).  
<sup>14</sup>M. S. Anand and R. P. Agarwala, *Trans. AIME* **239**, 1848 (1967).  
<sup>15</sup>K. Hirano, R. P. Agarwala, and M. Cohen, *Acta. Met.* **10**, 857 (1962).  
<sup>16</sup>T. S. Lundy and J. F. Murdock, *J. Appl. Phys.* **33**, 1671 (1962).  
<sup>17</sup>S. P. Murarka, M. S. Anand, and R. P. Agarwala, *Acta. Met.* **16**, 69 (1968).  
<sup>18</sup>R. P. Agarwala, S. P. Murarka, and M. S. Anand, *Acta. Met.* **12**, 871 (1964).  
<sup>19</sup>M. S. Anand, S. P. Murarka, and R. P. Agarwala, *J. Appl. Phys.* **36**, 3860 (1965).  
<sup>20</sup>J. E. Hilliard, B. L. Averbach, and M. Cohen, *Acta. Met.* **7**, 86 (1959).  
<sup>21</sup>D. E. Ovsienko and I. K. Zaslachuk, *Fiz. Metal. i Metalloved.* **10**, 743 (1960).  
<sup>22</sup>M. Beyeler, thesis, University of Paris, 1968 (unpublished).  
<sup>23</sup>T. Heuman and H. Böhmer, *J. Phys. Chem. Solids* **29**, 237 (1968).  
<sup>24</sup>T. J. Rowland and F. Y. Fradin, *Phys. Rev.* **182**, 760 (1969).  
<sup>25</sup>F. Y. Fradin and T. J. Rowland, *Appl. Phys. Letters* **11**, 207 (1967).  
<sup>26</sup>T. S. Lundy and J. F. Murdock, *J. Appl. Phys.* **33**, 1671 (1962).  
<sup>27</sup>T. G. Stoebe, R. D. Gulliver, T. O. Ogurtani, and R. A. Huggins, *Acta. Met.* **13**, 701 (1965).  
<sup>28</sup>P. E. Dougherty and R. S. Davis, *Acta. Met.* **7**, 118 (1959).  
<sup>29</sup>M. B. Kasen and D. H. Polonis, *Acta. Met.* **10**, 821 (1962).  
<sup>30</sup>J. R. Jasperse and P. E. Dougherty, *Phil. Mag.* **1**, 635 (1964).  
<sup>31</sup>B. K. Basu and C. Elbaum, *Acta. Met.* **13**, 1117 (1965).  
<sup>32</sup>M. B. Kasen, R. Taggart, and D. H. Polonis, *Phil. Mag.* **13**, 453 (1966).  
<sup>33</sup>D. Foss and O. H. Herbjørnsen, *Phil. Mag.* **13**, 945 (1966).  
<sup>34</sup>G. A. Chadwick, *Phil. Mag.* **14**, 1295 (1966).  
<sup>35</sup>O. H. Herbjørnsen and T. Astrup, *Phil. Mag.* **19**, 693 (1969).  
<sup>36</sup>T. R. Anthony, *Acta. Met.* **18**, 471 (1970).  
<sup>37</sup>B. K. Tarival and B. Ramaswami, *J. Appl. Phys.* (to be published).  
<sup>38</sup>R. O. Simmons and R. W. Balluffi, *Phys. Rev.* **117**, 52 (1960).  
<sup>39</sup>S. M. Edelglass and M. Ohring, *Trans. AIME* **245**, 186 (1969).  
<sup>40</sup>A. Blandin, J. L. Déplanté, and J. Friedel, *J. Phys. Soc. Japan Suppl.* **18**, 89 (1963).

## Infinite- $U$ Anderson Hamiltonian for Dilute Alloys\*

G. Toulouse<sup>†</sup>

*Department of Physics, University of California at San Diego, La Jolla, California 92037*

(Received 15 December 1969)

A Hamiltonian corresponding to the strictly infinite- $U$  limit of the Anderson Hamiltonian is considered. It is argued that this Hamiltonian retains enough complexity to describe magnetic and nonmagnetic impurities. The relationships with the Kondo Hamiltonian are discussed. A resolvent formula for the T-matrix elements, convenient for diagram expansions, is given. The characterization and the summation of the most divergent terms for the susceptibility and the spin-flip T-matrix element, in the magnetic and nonmagnetic regimes, are carried out and shown to be much simpler than for the Kondo Hamiltonian.

### I. INTRODUCTION

The interest in the dilute alloy problem is now focused on the nature of the low-temperature solution for the Kondo Hamiltonian<sup>1</sup> and on the transition regime between magnetic and nonmagnetic behavior for the Anderson Hamiltonian.<sup>2</sup> Evidence is given here that the study of a Hamiltonian, corresponding to the  $U \rightarrow \infty$  limit of the Anderson Hamiltonian, may shed some light on these two problems.

This Hamiltonian is<sup>3,4</sup>

$$H_M = \sum_{k\sigma} \epsilon_k n_{k\sigma} + E_d \sum_{\sigma} n_{\sigma} + V \sum_{k\sigma} (1 - n_{-\sigma}) [c_{k\sigma}^{\dagger} c_{\sigma} + c_{\sigma}^{\dagger} c_{k\sigma}] .$$

It is easily seen that  $[H_M, n_i] = 0$ , so that there are two independent subspaces corresponding to  $n_i = 0$  and  $n_i = 1$ ; the subspace  $n_i = 0$  is such that the double occupation of the  $d$  orbital is forbidden, which effectively corresponds to the limit  $U \rightarrow \infty$ .

For the full Anderson Hamiltonian, written in a transparent way as

$$H_A = h_0 + h_d + h_v + h_u ,$$

two typical choices of the perturbation term  $H_1$  can be made.

(a)  $H_1 = h_u$ , the Coulomb term. In this case the unperturbed Hamiltonian is quadratic and standard

Feynman diagrams can be used; the aim of such calculations,<sup>5</sup> so far, has been to study the transition magnetism-nonmagnetism by varying the ratio  $U/\Gamma$ , while keeping  $E_d/U$  fixed (generally taken as  $-\frac{1}{2}$ ). One drawback of such a procedure is that contact with calculations on the Kondo Hamiltonian does not easily come out.

(b)  $H_1 = h_v$ , the *mixing term*. In this case, for finite  $U$ , the unperturbed Hamiltonian is not quadratic and thus, the Wick theorem and standard perturbation theory do not apply. Equation-of-motion decoupling techniques are not the most convenient ones to study this model because the large- $U$  parameter enters in a nontrivial way<sup>6</sup>; however, taking infinite  $U$  from the onset, that is, starting from the Hamiltonian  $H_M$ , allows one to get rid of the major troubles. The Hamiltonian is still rich enough to study the transition from magnetism to nonmagnetism by varying  $E_d$ .<sup>4</sup> In this respect, it is probably safe to recognize that there may be significant differences between the transition region at  $E_d/U$  fixed and  $U$  variable and at  $U$  fixed and  $E_d$  variable. This last transition region is, however, more likely to be explored experimentally, because the position of the impurity orbital level relative to the Fermi energy can be varied by an applied pressure.<sup>7</sup>

Aside from those advantages concerning the study of the transition regime, the Hamiltonian  $H_M$  and its perturbation series possess some peculiar features which may make it even a better candidate than the Kondo Hamiltonian  $H_K$  for the study of the low-temperature magnetic regime.

## II. PERTURBATION FORMULAS

The quantities we shall be interested in are the most basic ones: ground-state energy  $E_B$ , partition function  $Z(T, H)$  and free energy as functions of temperature and magnetic field,  $d$  susceptibility, and  $T$ -matrix elements  $T(z, T)$  as functions of the incident energy and temperature.

For the calculation of these various quantities, there is no formal restriction to the use of Feynman diagrams. The unperturbed Hamiltonian is quadratic and the particles are all fermions. However, the use of the linked-cluster theorem implies that one should ignore the Pauli-principle restrictions when drawing the relevant connected diagrams; but, as the perturbation term at each step brings in the  $d$ -orbital annihilation or creation operators, effective account of the Pauli principle on this orbital allows one to eliminate a considerable fraction of the diagrams. Therefore, it appears preferable to give up the linked-cluster theorem and the Feynman diagrams and to use Goldstone diagrams, in time-dependent or resolvent formulations; this choice has the second

advantage of exhibiting a close relationship between  $H_M$  and the trivial Hamiltonian  $H_A^0$ , where

$$H_A^0 = \sum_k \epsilon_k n_k + E_d n + V \sum_k [c_k^\dagger c + c^\dagger c_k] ,$$

and between  $H_M$  and  $H_K$ .

### A. Partition Function and Vacuum Amplitude, Free Energy and Ground-State Energy

The partition function  $Z = \text{Tr} e^{-\beta H}$  gives all the thermodynamic quantities. As far as one is only interested in the ground-state energy, one may find it simpler to calculate the vacuum amplitude  $A = \langle 0 | e^{\beta H_0} e^{-\beta H} | 0 \rangle$ ,

$$\text{with } E_B - E_0 = - \lim_{\beta \rightarrow \infty} (1/\beta) \ln A(\beta) .$$

$Z$  and  $A$  are obtained as averages of the evolution operator  $U(\beta) = e^{\beta H_0} e^{-\beta H}$ ; the following formulas may be used:

(i) time-dependent formulas,

$$Z/Z_0 = 1 + \sum_{n=1}^{\infty} (-1)^n \int_0^\beta \dots \int_0^{u_{n-1}} \times \langle \mathcal{V}(u_1) \dots \mathcal{V}(u_n) \rangle du_1 \dots du_n , \quad (1)$$

$$A = 1 + \sum_{n=1}^{\infty} (-1)^n \int_0^\beta \dots \int_0^{u_{n-1}} \times \langle 0 | \mathcal{V}(u_1) \dots \mathcal{V}(u_n) | 0 \rangle du_1 \dots du_n ; \quad (2)$$

(ii) resolvent formulas,<sup>8</sup>

$$\frac{Z}{Z_0} = 1 - \beta \sum_{n=1}^{\infty} \frac{1}{n!} \text{Res}_{z=0} \frac{e^{-\beta z}}{z} \left\langle \mathcal{V} \left( \frac{1}{z - \delta H_0} \mathcal{V} \right)^{n-1} \right\rangle , \quad (3)$$

$$E_B - E_0 = \sum_{n=1}^{\infty} \frac{1}{n!} \text{Res}_{z=0} \frac{1}{z} \left\langle 0 \left| \mathcal{V} \left( \frac{1}{z - \delta H_0} \mathcal{V} \right)^{n-1} \right| 0 \right\rangle ; \quad (4)$$

(iii) Brillouin-Wigner formulas,<sup>9</sup>

$$\frac{Z}{Z_0} = \sum_q W_q e^{-\beta \eta_q} , \quad \eta_q = \sum_{n=1}^{\infty} \left\langle \mathcal{V} \left[ P \frac{1}{\eta_q - \delta H_0} \mathcal{V} \right]^{n-1} \right\rangle_q , \quad (5)$$

$$\Delta E_q = \sum_{n=1}^{\infty} \left\langle 0 \left| \mathcal{V} \left( P \frac{1}{E_q - \delta H_0} \mathcal{V} \right)^{n-1} \right| 0 \right\rangle , \quad (6)$$

where the index  $q$  refers to the unperturbed occupation of the extra-orbital levels and  $W_q$  is the unperturbed probability of these levels;  $\mathcal{V}$  and  $\mathcal{V}(u)$  refer to the interaction potential in Heisenberg and interaction representations.

Using the Wick theorem for the conduction electrons, all these formulas can be given Goldstone diagram representations. The rules of translation will differ from one formula to another, but the possible topological forms are identical. The resolvent formula for  $Z$  can be misleading if one does not correctly handle the accidentally vanishing energy denominators. On the other hand, in the presence of a dc magnetic field on the impurity orbital, there is a smaller number of singular diagrams for the susceptibility in the resolvent

formulation than in the time-dependent formulation. For each of these formulas the diagrams are the same for the Hamiltonians  $H_M$  and  $H_A^0$ ; the only difference comes from a numerical factor due to the spin degeneracy for  $H_M$ . Actually, this factor is  $2^c$ , where  $c$  is the number of connected parts of the diagram.

### B. $T$ Matrix

The  $T$ -matrix elements can be written in closed form, using the Schweber-Suhl formula,<sup>10</sup> but this form is not convenient for the use of diagram expansions. The diagrams defined by Brenig and Götze<sup>11</sup> apply for magnetic or ordinary scattering but cannot be used for the extra-orbital Hamiltonians.

The convenient expressions for such Hamiltonians can, in fact, be written in the resolvent way as

$$\langle \sigma, 0 | T(z) | \sigma, 0 \rangle = \sum_{n=1}^{\infty} (1/\phi) \text{Res}_{\rho=0} (1/\rho) \times \langle c_{k'\sigma} \mathcal{U} \{ [1/(\rho - \delta H_0)] \mathcal{U} \}^{n-1} c_{k\sigma}^\dagger \rangle_0, \quad \epsilon_k = \epsilon_{k'} = z \quad (7)$$

$$\langle \sigma', s | T(z) | \sigma, s \rangle = - \sum_{n=1}^{\infty} (1/\phi) \text{Res}_{\rho=0} (1/\rho) \times \langle c_{k'\sigma'} \mathcal{U} \{ [1/(\rho - \delta H_0)] \mathcal{U} \}^{n-1} c_{k\sigma}^\dagger \rangle_s. \quad (8)$$

Note that these formulas are valid at zero and finite temperature; just as in the formula of Sec. II A, the  $(1/\phi) \text{Res}_{\rho=0}$  term indicates how identically vanishing energy denominators must be handled. The corresponding diagrams have one entering and one leaving conduction-electron line; for the Hamiltonian  $H_A^0$ , there may be zero or one entering and leaving  $d$ -electron line; for the Hamiltonian  $H_M$ , three possibilities exist: zero, one spin up, one spin down, and four for the full Anderson Hamiltonian.

The plausibility of these formulas stems from two facts: (i) For  $H_A^0$ , one recovers the usual unambiguously defined one-body  $T$  matrix. (ii) For  $H_M$ , the perturbation expansion terms are identical to those obtained from a Schweber-Suhl formula.

### III. RELATION WITH KONDO HAMILTONIAN AND $E_d$ BIG NEGATIVE LIMIT

Similarities between the Kondo Hamiltonian and the extra-orbital Hamiltonian will be underlined by various methods, namely, canonical transformations, vacuum amplitudes, functional integral, and diagram techniques.

#### A. Canonical Transformations

Several authors, and in particular Schrieffer and Wolff,<sup>12</sup> have shown that up to second order in  $V$  the Anderson Hamiltonian contains an effective

spin-flip scattering term  $-J^{\text{eff}} \vec{S}_d \cdot \vec{S}(0)$ ,

where  $J^{\text{eff}} = 2V^2 u / E_d(E_d + U)$ ,

so that  $J^{\text{eff}} \rho = (2\Gamma/\pi) [U/E_d(E_d + U)]$  ;

for  $u$  infinite, one gets

$$J^{\text{eff}} \rho = 2\Gamma/\pi E_d.$$

These expressions are divergent for  $E_d = 0$ .

As a matter of fact, the canonical transformation which eliminates the mixing term produces four new terms (three for  $H_M$ ), among which are the preceding spin-flip term and an ordinary potential term, with matrix elements similar to  $J^{\text{eff}}$ . A second canonical transformation can be performed to eliminate this ordinary potential,<sup>13</sup> and one finally obtains a renormalized effective  $J_\perp$ , which no longer diverges for  $E_d = 0$  and whose asymptotic value for  $E_d \ll 0$  is  $J^{\text{eff}}$ .

#### B. Vacuum Amplitudes

The Anderson-Yuval approach<sup>14</sup> for the Kondo Hamiltonian, breaking the interaction into a longitudinal and a transverse part and calculating the vacuum amplitudes by perturbation in  $J_\perp$ , can be transposed to the Anderson Hamiltonian by using the following decomposition:  $H_A = H_0 + H_1$  with

$$H_0 = \sum_{k\sigma} \epsilon_k n_{k\sigma} + E_d \sum_{\sigma} n_{\sigma} + V \sum_k [c_k^\dagger c_\sigma + c_\sigma^\dagger c_{k\sigma}] + U n_\uparrow n_\downarrow,$$

$$H_1 = V \sum_k [c_{k\uparrow}^\dagger c_\uparrow + c_\uparrow^\dagger c_{k\uparrow}].$$

The underlying idea is to put the maximum number of terms in the unperturbed part while keeping it soluble, even at the expense of rotational symmetry, and then to use the Nozières-De Dominicis<sup>15</sup> expressions for each term of the perturbation series. It is easy to see that while the second-order term in  $J_\perp$  for  $H_K$  contained two x-ray transient responses contributing

$$[1/(\beta_1 - \beta_2)]^{2[1+(\delta_1 - \delta_2)/\pi]^2}$$

here, the second-order term in  $V$ , [formula (2)] will contain one unperturbed propagator (for spin-down electrons) and one "hole" transient response (for spin-up electrons) contributing

$$[1/(\beta_1 - \beta_2)]^{1+[ (\delta - \bar{\delta})/\pi ]^2} e^{-(\beta_1 - \beta_2)(E_d - \Delta E)},$$

for an unperturbed ground state containing no  $d$ , electron.  $\delta$  and  $\bar{\delta}$  are phase shifts at the Fermi level for the two following Hamiltonians of the  $H_A^0$  type:

$$H_0(n_i = 0) = \sum_k \epsilon_k n_k + E_d n + V \sum_k (c_k^\dagger c + c^\dagger c_k),$$

$$H_0(n_i = 1) = \sum_k \epsilon_k n_k + (E_d + U) n + V \sum_k (c_k^\dagger c + c^\dagger c_k),$$

and  $\Delta E$  is the difference in their respective ground-state energies

$$\Delta E = - (1/\pi) \int_{-\infty}^0 [\delta(E) - \bar{\delta}(E)] dE ,$$

where  $\delta(0) = \delta$ ,  $\bar{\delta}(0) = \bar{\delta}$ .

Practically,  $\delta$  and  $\bar{\delta}$  will be given by

$$\delta = \arccot(E_d/\Gamma), \quad \bar{\delta} = \arccot[(E_d + U)/\Gamma] ,$$

whereas  $E_d - \Delta E$  is such that (i) for  $|E_d|$ ,  $|E_d + U| < D$  width of the conduction band,

$$E_d - \Delta E \simeq \frac{\Gamma}{\pi} \left[ \frac{E_d}{\Gamma} \arccot\left(-\frac{E_d}{\Gamma}\right) + \frac{E_d + U}{\Gamma} \times \arccot\left(\frac{E_d + U}{\Gamma}\right) + \frac{1}{2} \ln\left(\frac{\Gamma^2 + (E_d + U)^2}{\Gamma^2 + E_d^2}\right) \right] ;$$

(ii) for  $U$  infinite,

$$E_d - \Delta E \simeq \frac{\Gamma}{\pi} \left[ \frac{E_d}{\Gamma} \arccot\left(-\frac{E_d}{\Gamma}\right) + 1 + \frac{1}{2} \ln\left(\frac{D^2}{\Gamma^2 + E_d^2}\right) \right] .$$

More generally, the  $2n$ th-order term will contain a determinant of free propagators with the exponent  $1 + (\delta - \bar{\delta}/\pi)^2$  multiplied by the term

$$\exp\left((E_d - \Delta E) \sum_{i=1}^{2N} (-1)^i \beta_i\right) .$$

Following Anderson-Yuval<sup>14</sup> and taking advantage of the particular features of Cauchy determinants, this problem can be related to a one-dimensional problem of charged classical hard-core particles interacting with a logarithmic potential *and* in the presence of an electric field, or to a one-dimensional Ising problem with a  $1/n^2$  interaction *and* in the presence of a magnetic field. In both equivalent problems, the “inverse temperature” is proportional to the exponent

$$T^{-1} = 1 + [(\delta - \bar{\delta})/\pi]^2 ,$$

and the “external field” is proportional to the coefficient  $(E_d - \Delta E)$ . We shall discuss successively these two parameters.

### 1. Inverse Temperature

The range of “inverse temperatures” is clearly

$$1 \leq T^{-1} \leq 2 ,$$

whereas, for the Kondo Hamiltonian, the range is (with  $\delta_1 = -\delta$ ,  $\delta_1 = \arctan \frac{1}{4} \pi J_{z0}$ )

$$0 \lesssim T^{-1} \lesssim 8 .$$

The restricted range on the “low-temperature” side ( $T^{-1} = 2$ ) reflects the fact that the Anderson Hamiltonian can never describe an impurity with a ferromagnetic coupling to the conduction electrons; the restricted range on the “high-temperature” side ( $T^{-1} = 1$ ) is instructive also, as it is known<sup>14,16</sup> that the Kondo problem is “soluble” for the particular corresponding value of  $J_z$ .  $T^{-1}$  is a function of  $\Gamma/U$  and  $E_d/U$ ,

$$T^{-1} = 1 + ((1/\pi) \arccot\{[E_d(E_d + U) + \Gamma^2]/\Gamma U\})^2 ,$$

from which an expression for an “effective”  $J_z$  can be obtained, where

$$J_z \simeq (4/\pi\rho) \tan\left\{\frac{1}{2}\pi\left[\left(\frac{1}{2}T^{-1}\right)^{1/2} - 1\right]\right\} . \quad (9)$$

It should be noted that the “effective”  $J_z$  value is determined by a comparison of ground-state energies only and, as a matter of fact, only part of the ground-state energies, since the unperturbed Hamiltonians contain part of the coupling constants. Such a comparison may lead from an isotropic Anderson Hamiltonian to an anisotropic effective  $J$ , which can only make sense for ground-state energy values. In the limit  $(-E_d/\Gamma \gg 1, E_d + U/\Gamma \gg 1)$  formula (9) leads to a  $J_z$  value which is half the Schrieffer-Wolff expression.

### 2. External Field

It is easily seen that in the symmetric case,  $2E_d + U = 0$ , and the “external field” vanishes; in fact, the external field is an odd function of the variable  $E_d + U/2$ , which asymptotically tends to  $2E_d + U$  when  $|E_d| \rightarrow \infty$ . Similarly, in the  $U$ -strictly-infinite limit, as  $E_d$  increases from  $-\infty$  to  $+\infty$ , the external field rises monotonically from zero to an asymptotic value equal to  $E_d$ . One may argue physically that such a constant external field is likely to damp the fluctuations and to suppress any criticallike behavior in the Anderson problem, as in the related classical particles or Ising problems.

### C. Functional Integrals

The following considerations are of rather formal interest and we shall not insist on them, since any real calculation seems remote; however, they may provide some guiding thoughts.

The functional integral method of Stratonovitch<sup>17</sup> relates the partition function of the Hamiltonian  $H = H_0 - \lambda^2 H_1^2$  to an average of partition functions for the family of time-dependent Hamiltonians

$$H(\tau) = H_0 + \lambda(\tau) H_1 .$$

The idea is then to go the reverse way by squaring the mixing term  $V_M$  of the Hamiltonian  $H_M$ . The result is the following. Consider the Hamiltonian  $\tilde{H}$ :

$$\begin{aligned} \tilde{H} &= \sum_{k\sigma} \epsilon_k n_{k\sigma} + E_d(n_+ + n_-) + (\tfrac{1}{2}J) \mathbf{V}_M^2 \\ &= \sum_{k\sigma} \epsilon_k n_{k\sigma} + E_d(n_+ + n_-) + (\tfrac{1}{2}J) \{-2\vec{S}_d \cdot \vec{S}(0) \\ &\quad + (n_+ - n_-)^2 + [(1 - n_+)(1 - n_-) - \tfrac{1}{2}(n_+ - n_-)^2] \\ &\quad \times \sum_{kk'\sigma} c_{k\sigma}^\dagger c_{k'\sigma}\} . \end{aligned}$$

This Hamiltonian commutes with  $n_+ + n_-$ ; its expressions in the three corresponding subspaces are



FIG. 1. Sixth-order diagram for the  $T$  matrix.

$$\tilde{H}_0 = \sum_{k\sigma} \epsilon_k n_{k\sigma} + \frac{1}{2} J \sum_{kk'\sigma} c_{k\sigma}^\dagger c_{k'\sigma}, \quad (n_i + n_i = 0)$$

$$\tilde{H}_1 = \sum_{k\sigma} \epsilon_k n_{k\sigma} + E_d - J \tilde{S}_d \cdot \tilde{S}(0) + \frac{1}{2} J - \frac{1}{4} J \sum_{kk'\sigma} c_{k\sigma}^\dagger c_{k'\sigma}, \quad (n_i + n_i = 1)$$

$$\tilde{H}_2 = \sum_{k\sigma} \epsilon_k n_{k\sigma} + 2E_d \quad (n_i + n_i = 2).$$

$\tilde{H}_0$  and  $\tilde{H}_2$  are trivially soluble Hamiltonians;  $\tilde{H}_1$  is essentially a Kondo Hamiltonian with an ordinary potential term added.

The partition function of the total Hamiltonian  $\tilde{H}$  is

$$\tilde{Z} = Z_0 \langle T \exp \{ -\frac{1}{2} J \int_0^\beta [\tilde{v}_M(\tau)]^2 d\tau \} \rangle,$$

which can be cast into integral functional form as

$$\tilde{Z} = Z_0 \int \mathcal{D}x(\tau) \langle T \exp \{ - \int_0^\beta d\tau [(\pi/\beta)x^2(\tau) + (-2\pi J/\beta)^{1/2} x(\tau) \tilde{v}_M(\tau)] \} \rangle,$$

or with obvious notations

$$\tilde{Z} = [Z_n(x)]_x. \quad (10)$$

Now, admittedly, we have not achieved much here, since one generally tries to reduce a many-body problem to an average of one-body problems, and we have not done that. Formula (10) is only a formal exact relation between the Kondo and Anderson ( $U\infty$ ) Hamiltonians.

#### D. Diagrams

Let us consider the  $T$ -matrix diagrams for the Hamiltonian  $H_M$ . A typical sixth-order diagram is depicted in Fig. 1, where full lines represent conduction-electron propagators and dotted lines the  $d$ -electron propagators. The Pauli principle and the projection operators in  $V_M$  prevent two dotted lines from running at the same time. One out of two successive energy denominators will contain  $E_d$ . In the limit of  $E_d$  big negative, one may wish to neglect all conduction-electron energies in those denominators containing  $E_d$  (this is, in fact, our definition of  $E_d$  big negative); then the diagram of Fig. 1 may be reduced to the form of Fig. 2, with a new interaction which is easily seen

to be

$$\bar{v} = -\frac{V^2}{E_d} \sum_{kk'\sigma} [c_{k\sigma}^\dagger c_{k'\sigma} c_{-\sigma} c_{-\sigma}^\dagger + c_{k\sigma}^\dagger c_{k'\sigma} c_{-\sigma}^\dagger c_{\sigma}] \quad (11)$$

(For  $H_A^0$ , it would be  $-V^2/E_d \sum_{kk'} c_{k\sigma}^\dagger c_{k'\sigma}$ .) Formula (11) can also be written as

$$\bar{v} = -\frac{2V^2}{E_d} \tilde{S}_d \cdot \tilde{S}(0) - \frac{V^2}{E_d} [1 - \frac{1}{2}(n_i + n_i)] \sum_{kk'\sigma} c_{k\sigma}^\dagger c_{k'\sigma}. \quad (12)$$

In the subspace  $n_i + n_i = 1$ , this interaction takes the particular form

$$\bar{v} = -\frac{V^2}{E_d} \sum_{kk'\sigma\sigma'} c_{k\sigma}^\dagger c_{k'\sigma'} c_{\sigma'}^\dagger c_{\sigma} \quad (13)$$

$$= -\frac{2V^2}{E_d} \tilde{S}_d \cdot \tilde{S}(0) - \frac{V^2}{2E_d} \sum_{kk'\sigma} c_{k\sigma}^\dagger c_{k'\sigma}. \quad (14)$$

Formula (12) is closely related to the Schrieffer-Wolff result; however, the Schrieffer-Wolff result is, in some sense, both more general and more restricted. It is more general because the obtained effective  $J$  value has a dependence on  $\epsilon_k \epsilon_{k'}$ , and more restricted because it is only valid in second order in  $V$  (one might expect other spin-flip terms in higher order from the canonical transformation). The Hamiltonian  $H_L$ , defined, for instance, as

$$H_L = \sum_{k\sigma} \epsilon_k n_{k\sigma} + \lambda_1 \sum_{\sigma} n_{\sigma} + \lambda_2 \sum_{kk'\sigma\sigma'} c_{k\sigma}^\dagger c_{k'\sigma'} c_{\sigma'}^\dagger c_{\sigma} \quad (15)$$

is a perfectly respectable, rotationally invariant Hamiltonian which may be considered without any reference to the Anderson Hamiltonian. To help visualize its connection with the Kondo Hamiltonian, we give in Table I the matrix elements  $\langle s, \sigma | V | s', \sigma' \rangle$ , where  $s$  is the  $d$ -electron spin and  $\sigma$  a conduction-electron spin.

This concludes our general considerations; Sec. IV is devoted to the diagrammatics for  $H_M$  and  $H_L$ , and in particular, to the determination of the most divergent diagrams.

#### IV. SUMMATION OF THE MOST DIVERGENT TERMS

We shall concentrate on the  $d$  susceptibility and the  $T$  matrix, which are the most interesting quantities in the dilute alloy problem.



FIG. 2. Reduced diagram in the  $E_d$  big negative limit.

TABLE I. Matrix elements of the interaction for the Hamiltonians  $H_K$  and  $H_L$ .

$s\sigma$	$\uparrow\uparrow$	$\uparrow\downarrow$	$\downarrow\uparrow$	$\downarrow\downarrow$		$s\sigma$	$\uparrow\uparrow$	$\uparrow\downarrow$	$\downarrow\uparrow$	$\downarrow\downarrow$
$\uparrow\uparrow$	1					$\uparrow\uparrow$	1			
$\uparrow\downarrow$		-1	2			$\uparrow\downarrow$		1		
$\downarrow\uparrow$		2	-1			$\downarrow\uparrow$		1		
$\downarrow\downarrow$				1		$\downarrow\downarrow$			1	
$H_K$						$H_L$				

## A. Susceptibility

A magnetic field is applied on the  $d$  orbital, introducing in the unperturbed Hamiltonian a term  $\mu H(n_{\uparrow} - n_{\downarrow})$ , which can be lumped into  $\sum_{\sigma} E_d^{\sigma} n_{\sigma}$  with  $E_d^{\sigma} = E_d + \sigma \mu H$ ,  $\sigma = \pm 1$ . Formula (5) is used for the partition function together with the expression

$$\Delta\chi_{dd} = \frac{1}{\beta} \frac{1}{Z/Z_0} \left. \frac{\partial^2 (Z/Z_0)}{\partial H^2} \right|_{H=0}.$$

The first divergent contribution appears in fourth order in  $V$  (Fig. 3), for one diagram out of four. Its contribution to  $Z$  is

$$\beta V^4 \sum_{12\sigma} \frac{(1-f_1)f_2}{(\epsilon_1 - E_d^{\sigma})^2 (\epsilon_1 - \epsilon_2 + 2\sigma\mu H)} \langle n_{\sigma} \rangle,$$

and its contribution to  $\Delta\chi_{dd}$  is

$$-4\langle n \rangle \frac{\mu^2}{T} V^4 \sum_{12\sigma} \frac{(1-f_1)f_2}{(\epsilon_1 - E_d^{\sigma})^2 (\epsilon_1 - \epsilon_2)^2},$$

or in the  $E_d$  big negative limit

$$(\mu^2/T)(2V^2/E_d)^2 \ln(T/D).$$

Now it can be seen that the most divergent contribution in  $2n$ th order is obtained from the one diagram with  $(n-1)$  loops inserted; for example, in sixth order in  $V$ , one diagram (Fig. 4) out of twelve is contributing, whereas for the Kondo Hamiltonian, in third order in  $J$ , the two diagrams contribute. The series of most divergent contributions is a geometric series, which is easily resummed as

$$\frac{Z}{Z_0} = 1 + \beta V^2 \sum_{1\sigma} \left[ (1-f_1) \langle n_{\sigma} \rangle \times \left( \epsilon_1 - E_d^{\sigma} - V^2 \sum_{2\sigma} \frac{f_2}{\epsilon_1 - \epsilon_2 + (\sigma - \sigma')\mu H} \right)^{-1} \right],$$

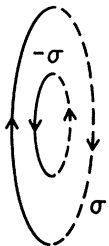


FIG. 3. Fourth-order diagram for the partition function.



FIG. 4. Sixth-order diagram for the partition function.

giving for  $\Delta\chi_{dd}$

$$\begin{aligned} \Delta\chi_{dd} &= -4\langle n \rangle \frac{\mu^2}{T} V^2 \sum_1 \left[ (1-f_1) \right. \\ &\quad \times \left( \epsilon_1 - E_d - 2V^2 \sum_2 \frac{f_2}{\epsilon_1 - \epsilon_2} \right)^{-2} \Big] \\ &\quad \times \left[ 1 + 2V^2 \sum_2 \left( \frac{f_2}{(\epsilon_1 - \epsilon_2)^2} \right) \right] \\ &= 2 \frac{\mu^2}{T} \langle n \rangle \frac{2V^2 \rho}{E_d - 2V^2 \rho \ln(T/D)}, \end{aligned}$$

where a rectangular band of density  $\rho$  and width  $2D$  has been assumed; the limit  $E_d$  big negative merely turns  $\langle n \rangle$  into  $\frac{1}{2}$ .<sup>18</sup>

Two points should be noticed: (i) One and only one diagram contributes the most divergent term in each order. (ii) The corresponding geometric series can be summed for general  $E_d$ .

B.  $T$  Matrix

The matrix elements

$$\langle \sigma, 0 | T(z) | \sigma, 0 \rangle$$

do not, as expected, contribute divergent terms, so we shall concentrate on the matrix elements

$$T_{,,} = \langle \sigma, \sigma | T(z) | \sigma, \sigma \rangle$$

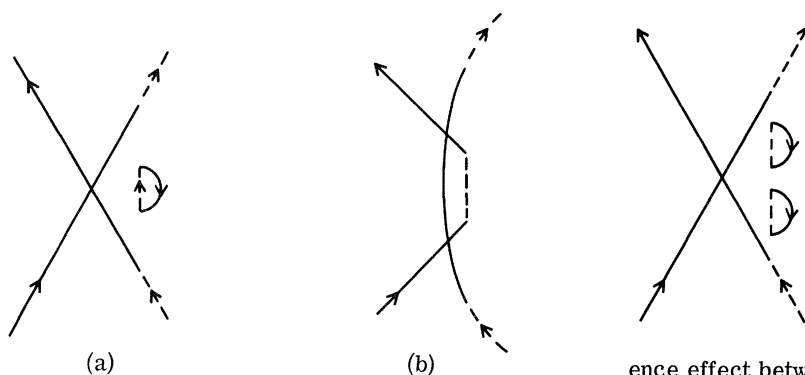
$$\text{and } T_{,,} = \langle \sigma, -\sigma | T(z) | \sigma, -\sigma \rangle,$$

from which the forward and spin-flip amplitudes are obtained as

$$T_{nsf} = \frac{1}{2}(T_{,,} + T_{,,}), \quad \tau = \frac{1}{2}(T_{,,} - T_{,,}).$$

From the definition (8), it can be seen that diagrams for  $T_{,,}$  and  $T_{,,}$  are obtained from those diagrams for  $Z/Z_0$ , with one backward running  $d$ -electron line, by opening that  $d$ -electron line and one conduction-electron line; Fig. 5 shows the diagrams obtained from the particular partition function diagram of Fig. 3. Diagram (a) contributes with a factor of 2 (due to the spin counting of the closed loop) to  $T_{,,}$ , and diagram (b) contributes with the same factor to  $T_{,,}$  and  $T_{,,}$ , so that contribution to  $\tau$  comes only from diagram (a).

A particular class of partition function diagrams ( $C_1$ ) has been seen to contribute the most divergent

FIG. 5. Fourth-order diagrams for the  $T$  matrix.

terms for the susceptibility. Now it can be seen that for  $\tau$  partial cancellation occurs in such a way that the most divergent part is given by those diagrams which are constructed from class  $C_1$ . These are, in fact, diagrams (one in each order) containing the maximum number of loops, such as diagram (a) of Fig. 5 or the sixth-order diagram of Fig. 6.

Now, this class of  $T$ -matrix diagrams gives rise to a geometric series which is easily summed as

$$2\tau(z) = V^2 / \left( z - E_d - 2V^2 \sum_1 \frac{f_1}{z - \epsilon_1} \right),$$

or at zero temperature as

$$2\tau(z) = \frac{V_2}{z - E_d + 2V^2 \ln(z/D)}.$$

Again, it should be noted that (i) one and only one diagram gives the most divergent term for  $\tau$  in each order, and this class of diagrams is directly obtained from the class  $C_1$  of singular diagrams for  $\chi_{ad}$  (diagrams with the biggest number of closed loops). This is a striking result if one goes to the  $E_d$  big negative limit where diagrams of the type of Fig. 2, similar to the Brenig-Götze diagrams for  $H_K$ , can be used. Compared to  $H_K$ , there occurs for  $H_L$  a kind of coher-

FIG. 6. Sixth-order diagram for the  $T$  matrix.

ence effect between the spin-flip scattering and the ordinary scattering which reduces the burden of summing "parquet" graphs<sup>19</sup> or "one-particle intermediate states" graphs<sup>17</sup> to the simple task of performing a geometric bubble-series summation. (ii) The summation is valid for general  $E_d$ .

## V. DISCUSSION

Summing the most divergent terms is only a first step. The Nagaoka-Suhl approximation achieves that in addition to the requirement of good analytical properties for the  $T$  matrix. It is particularly clear in the diagrammatic formulation of Brenig and Götze for  $H_K$  that this approximation retains one family of the next divergent diagrams and neglects totally another one, i. e., disconnected diagrams containing information on the spin memory. This drawback is now widely recognized and attempts have been made to build a "renormalized parquet" graph theory<sup>20</sup> in order to include such spin-memory effects.

The results presented here strongly indicate that this second step should be carried out on  $H_M$  rather than on  $H_K$ , since the first step was easier on  $H_M$ .

## ACKNOWLEDGMENTS

Numerous discussions with A. Blandin and C. De Dominicis are gratefully acknowledged. The author wishes to thank Professor H. Suhl for his hospitality at the University of California, San Diego, during the final stage of this work.

\*Work sponsored in part by the Air Force Office of Scientific Research, U. S. Air Force, under Grant No. AF-AFOSR-610-67.

<sup>†</sup>On leave of absence from the Service de Physique des Solides, Faculté des Sciences, 91, Orsay, France.

<sup>1</sup>J. Kondo, *Solid State Phys.* **23**, 184 (1970).

<sup>2</sup>P. W. Anderson, in *Many-Body Physics*, edited by C. De Witt and R. Balian (Gordon and Breach, New York, 1968), p. 229.

<sup>3</sup>A. Blandin, J. Perrier, and G. Toulouse, *Compt. Rend.* **265B**, 719 (1967).

<sup>4</sup>G. Toulouse, thesis, Orsay, 1968 (unpublished).

<sup>5</sup>J. R. Schrieffer and D. C. Mattis, *Phys. Rev.* **140**, 1412 (1965); D. R. Hamann, *ibid.* **186**, 549 (1969).

<sup>6</sup>L. Dworin, *Phys. Rev.* **164**, 818 (1968); **164**, 841 (1968).

<sup>7</sup>M. B. Maple and Kang-Soo Kim, *Phys. Rev. Letters* **23**, 118 (1969); M. B. Maple, J. Wittig, and Kang-Soo

Kim, *ibid.* **23**, 1375 (1970).

<sup>8</sup>C. Bloch and C. De Dominicis, Nucl. Phys. **7**, 459 (1963).

<sup>9</sup>C. De Dominicis and G. Toulouse, Physica (to be published).

<sup>10</sup>H. Suhl, Phys. Rev. **138**, 515 (1965).

<sup>11</sup>W. Brenig and W. Götze, Z. Physik **217**, 188 (1968).

<sup>12</sup>J. R. Schrieffer and P. A. Wolff, Phys. Rev. **149**, 491 (1966).

<sup>13</sup>G. Toulouse and B. Coqblin, Solid State Commun. **7**, 853 (1969).

<sup>14</sup>P. W. Anderson and G. Yuval, Phys. Rev. Letters **23**, 89 (1969); G. Yuval and P. W. Anderson, Phys. Rev.

B **1**, 1522 (1970); P. W. Anderson, G. Yuval, and D. R. Hamann (report of work prior to publication).

<sup>15</sup>P. Nozières and C. De Dominicis, Phys. Rev. **178**, 1097 (1969).

<sup>16</sup>G. Toulouse, Compt. Rend. **268**, 1200 (1969); **268**, 1257 (1969).

<sup>17</sup>R. L. Stratonovitch, Dokl. Akad. Nauk. SSSR **115**, 1097 (1957) [Soviet Phys. Doklady **2**, 416 (1958)].

<sup>18</sup>D. J. Scalapino, Phys. Rev. Letters **16**, 937 (1966).

<sup>19</sup>A. A. Abrikosov, Physics **2**, 5 (1965).

<sup>20</sup>P. Nozières, J. Gavoret, and B. Roulet, Phys. Rev. **178**, 1084 (1969).

## Long-Range Order in $\beta$ Brass

J. C. Norvell\* and J. Als-Nielsen†

*Physics Department, Research Establishment Risø, The Danish Atomic Energy Commission, Roskilde, Denmark*

(Received 18 February 1970)

The long-range order parameter  $M$  of  $\beta$  brass has been determined from measurements of the intensity of superlattice reflections of Bragg-scattered neutrons. Over the whole temperature range  $T=300^\circ\text{K}$  to  $T=T_c=736^\circ\text{K}$ , the data are in remarkable agreement with the prediction for the compressible Ising bcc lattice with only nearest-neighbor interactions.

### I. INTRODUCTION

The alloy  $\beta$  brass is composed of approximately equal parts of Cu and Zn. At room temperature the cube corners of the bcc lattice are predominantly occupied by one type of atom – say Cu atoms – and the centers by Zn atoms. As the temperature is raised, the occupation of lattice sites becomes more and more random, until at the critical temperature  $T_c$  the average occupation of a lattice site is entirely random. Even above  $T_c$ , however, the occupation of lattice sites is correlated in the sense that if a certain site is occupied by a Cu atom, there will be an excess probability over randomness that the nearest-neighbor sites are occupied by Zn atoms and so on. The occupation of lattice sites can be studied by a diffraction experiment and in this paper we describe a measurement of the average occupation of a lattice site below  $T_c$ . This average occupation of a lattice site is a measure of the long-range order and corresponds to the magnetization in an Ising magnet. In an earlier study, Chipman and Warren<sup>1</sup> examined the long-range order in  $\beta$  brass by x-ray diffraction.

It has been emphasized previously that the order-disorder transition in  $\beta$  brass provides an exceptional possibility for an accurate comparison between experiment and a relevant theory for phase

transitions. This is because the configurational energy in the alloy is formally given by the Ising-magnet Hamiltonian, a model which is sufficiently simple to allow detailed theoretical calculations. Indeed, previous neutron scattering experiments have verified the theoretical predictions for the correlation range and the temperature dependence of the magnetization and of the susceptibility.<sup>2-4</sup> As we shall see, the results of the present experiment on the average occupation of a lattice site are also in very good agreement with theory.

The Bragg-scattering cross section  $(d\sigma/d\Omega)_B$  for a superlattice reflection from a rigid lattice is

$$\left(\frac{d\sigma}{d\Omega}\right)_B = \frac{1}{4} N^2 (f_{\text{Cu}} - f_{\text{Zn}})^2 M^2 \delta(\vec{K} - \vec{\tau}) \quad (1)$$

Here  $N$  is the number of atoms in the single-crystal sample, and  $f_{\text{Cu}}$  and  $f_{\text{Zn}}$  the scattering amplitudes of Cu and Zn atoms, respectively. The scattering vector  $\vec{K}$  is the difference between the incident and scattered neutron wave vectors,  $\vec{\tau}$  is a reciprocal superlattice vector, i.e., a vector in reciprocal space with an odd sum of indices, and  $M$  gives the average occupation of a lattice site. Let  $S_i$  be defined as +1 if the lattice site at position  $\vec{r}_i$  is occupied by a Cu atom and -1 if it is occupied by a Zn atom, then  $M = \langle \sum_i S_i e^{i\vec{\tau} \cdot \vec{r}_i} \rangle$ . The temperature dependence of  $M$  near  $T_c$  can be expressed by the power law